Journal of Power Sources 216 (2012) 387–394

Contents lists available at SciVerse ScienceDirect

Journal of Power Sources

journal homepage: www.elsevier.com/locate/jpowsour

Sulfonated block-graft copolyimide for high proton conductive and low gas permeable polymer electrolyte membrane

Kota Yamazaki, Gang Wang, Manabu Tanaka, Hiroyoshi Kawakami*

Department of Applied Chemistry, Tokyo Metropolitan University, Hachioji, Tokyo 192 0397, Japan

HIGHLIGHTS

- A series of sulfonated block and/or graft polyimides were synthesized.
- The S-*bg*-PI membrane showed higher proton conductivity than Nafion and other SPI membranes.
- Oxygen permeability of the S-*bg*-PI membrane was much lower than those of other membranes.
- The novel S-*bg*-PI membrane with excellent properties is expected for fuel cell applications.

GRAPHICAL ABSTRACT

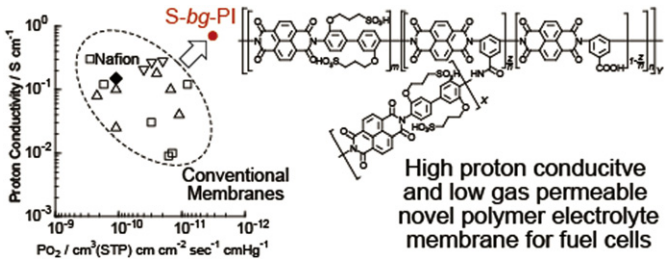

ARTICLE INFO

Article history:
Received 7 March 2012
Received in revised form
15 May 2012
Accepted 28 May 2012
Available online 5 June 2012

Keywords:
Fuel cell
Polymer electrolyte
Proton conductivity
Gas permeability

ABSTRACT

This paper addresses issues surrounding the design of the proton exchange membrane for fuel cells, and more specifically, the role of the polymer architecture on the proton conductivity and gas permeability. In this study, we describe the syntheses and characterizations of sulfonated block, graft, random-graft, and block-graft copolymers. The proton conductivity and oxygen permeability of the novel sulfonated block-graft copolyimide, S-*bg*-PI, showed 0.44 S cm^{-1} at 80 °C and 98%RH and 3.2 × 10^{-12} cm^3(STP) cm/(cm^2 sec cmHg) at 35 °C and 76 cmHg, respectively, while those of Nafion indicated 0.15 S cm^{-1} and 1.1 × 10^{-10} cm^3(STP) cm/(cm^2 sec cmHg) under the same conditions, respectively. The apparent selectivity ratio calculated from the proton and oxygen transports of S-*bg*-PI was 103 times larger than that determined in Nafion, indicating that the novel sulfonated block-graft copolyimide membrane has excellent properties for fuel cell applications.

1. Introduction

Future polymer electrolyte fuel cells (PEFCs) will be operated under low humidity or dry conditions to reduce the system cost, therefore, effective water management within the cell will be very important [1–3]. One approach to solve these problems is to reduce the thickness of the proton exchange membrane (PEM) for fuel cells [4]. PEM is one of the key components in PEFCs, and requires various properties including high proton conductivity, high chemical and physical stability, and low gas permeability [5–7]. Reducing the thickness promises to achieve higher levels of proton conduction concerned with a higher power density, and will facilitate the water back diffusion, which is a spontaneous water transfer phenomenon from the cathode to the anode due to concentration gradient of water in the membrane [4,7–9]. This reduction, however, increases the risks with respect to its mechanical strength and gas permeability. In particular, hydrogen and oxygen crossovers through the membrane are undesirable diffusion, because their crossovers lead to at least three problems, *i.e.*, fuel efficiency reduction, cell potential depression, and formation of reactive oxygen species (ROS), which are believed to attack

* Corresponding author. Tel.: +81 426 77 1111x4972; fax: +81 426 77 2821.
E-mail addresses: tanaka-manabu@tmu.ac.jp (M. Tanaka), kawakami-hiroyoshi@tmu.ac.jp (H. Kawakami).

0378-7753/$ – see front matter © 2012 Elsevier B.V. All rights reserved.
http://dx.doi.org/10.1016/j.jpowsour.2012.05.097

not only the catalyst but also the membrane causing a significant degradation of catalyst-layer and membrane [10–12]. The roles of the polymer architecture on its properties, such as proton conductivity and gas permeability, are still poorly understood. Recently, we revealed that polymer architecture, for example graft polymer structures, helped enhancement of proton conductivity and suppression of gas permeability [13]. Taking this idea one step further, this paper addresses issues surrounding the design of the PEM for fuel cells, and more specifically the role of the polymer architecture, including block, graft, random-graft, and block-graft structures, on the proton conductivity and gas permeability. We now describe the syntheses and characterizations of sulfonated block (S-*b*-PI), graft (S-*g*-PI), random-graft (S-*rg*-PI), and block-graft (S-*bg*-PI) copolyimides. The chemical structures of the series of sulfonated copolyimides are summarized in Fig. 1, and the frame formats of these polymers are also illustrated to help recognizing the differences among the polymer architectures. The four series are designed to possess similar IEC values, but considerably different architectures to systematically understand the relationships between the chemical structure of polymers and their fuel cell property. Their proton conductivities, gas permeabilities, and proton/oxygen transport selectivity were discussed as well as their chemical stabilities.

2. Experimental

2.1. Materials

1,4,5,8-Naphthalene tetracarboxylic dianhydride (NTDA) and 3.5-diaminobenzoic acid (DABA) were purchased from the Sigma–Aldrich Co. (St. Louis, MO, USA) and were used as received. 3,3′-Bis(3-sulfo-propoxy) benzidine (BSPB) was prepared using the same method reported by Watanabe et al. [14]. 2,2-Bis[4-(4-aminophenoxy)phenyl]-hexafluoropropane (APPF) was purchased from the Wako Pure Chemical Industries Co. (Osaka, Japan) and was recrystallized twice from an ethanol solution prior to use. All other

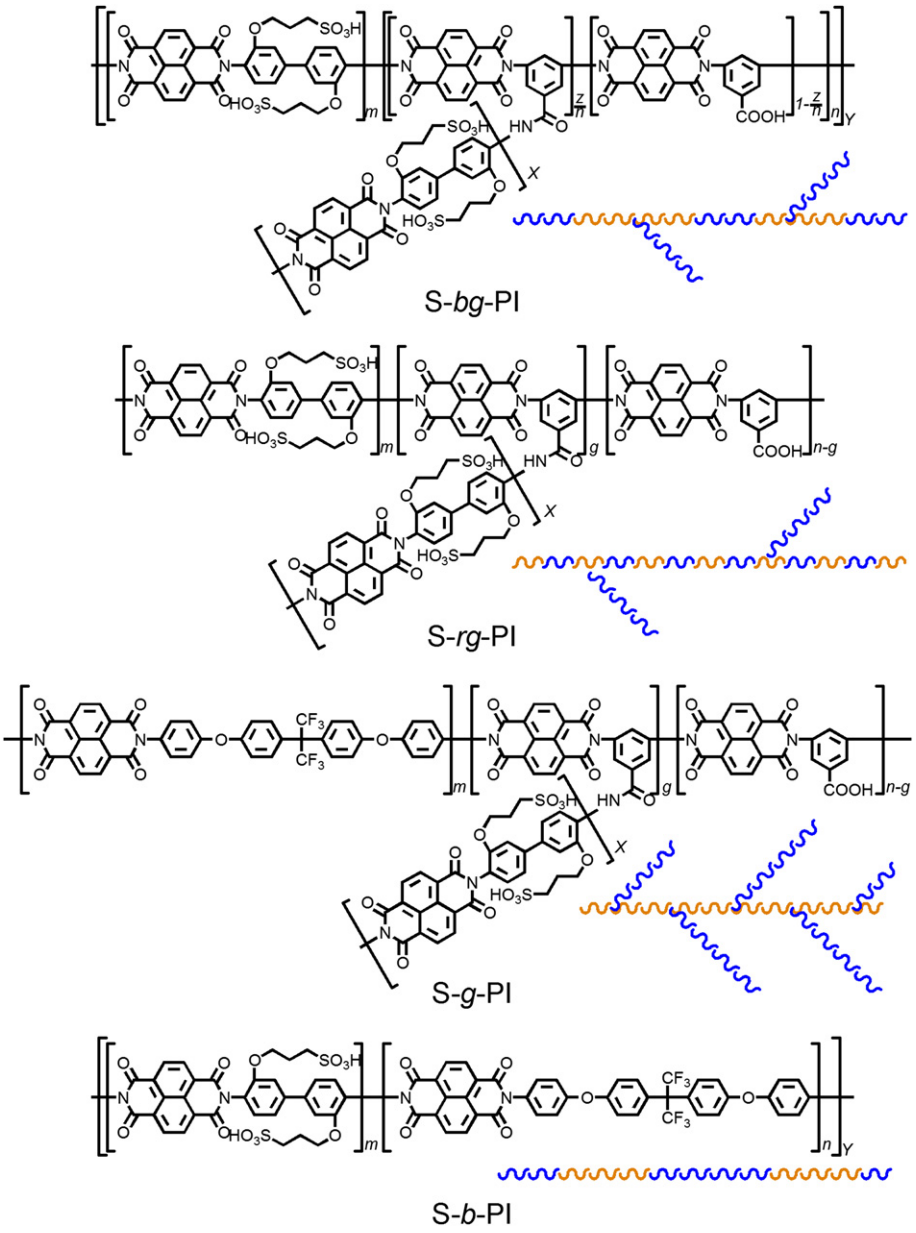

Fig. 1. Chemical structures of sulfonated copolyimides.

chemicals were purchased from Kanto Chemical Co. (Tokyo, Japan) and were used as received. Nafion® 117 was used in this study as the control membrane. The membranes were obtained from the DuPont Co. Ltd. (Tokyo, Japan).

2.2. Synthesis of sulfonated block-graft copolyimide (S-bg-PI)

A novel sulfonated block-graft copolyimide was synthesized as shown in Scheme 1. The main-chain polymer, NTDA-BSPB-*b*-DABA, and the side-chain polymer, NTDA-BSPB, were synthesized using the same method reported in our previous paper [13]. The synthesis of NTDA-BSPB-*b*-DABA as the main-chain polymer was carried out as follows: The diamine-terminated hydrophilic polyimide, NTDA-BSPB, was prepared by the reaction of NTDA (1.45 g, 5.42 mmol) and the excess of BSPB (2.53 g, 5.49 mmol) in *m*-cresol (25 ml) in the presence of triethylamine (TEA, 2.4 ml) at 120 °C for 24 h, and the dianhydride-terminated hydrophobic polyimide, NTDA-DABA, was prepared by the reaction of DABA (0.36 g, 2.36 mmol) and the excess of NTDA (0.65 g, 2.44 mmol) in *m*-cresol (10 ml) in the presence of TEA (1.0 ml) at 120 °C for 24 h. The BSPB/DABA mol% was 70/30. After 24 h, the diamine-terminated polyimide solution was added to the dianhydride-terminated polyimide to synthesize NTDA-BSPB-*b*-DABA as the sulfonated block copolyimide. After a 180 °C reaction for 24 h, the NTDA-BSPB-*b*-DABA was precipitated in ethyl acetate, washed several times with fresh ethyl acetate, and recovered. Subsequently, the NTDA-BSPB-*b*-DABA was dried in a vacuum oven at 150 °C for 15 h. The sulfonated block-graft copolyimide, S-*bg*-PI, was synthesized from the NTDA-BSPB-*b*-DABA as the main-chain polymer and the NTDA-BSPB as the side-chain polymer with triphenylphosphine as a condensation reagent in the presence of pyridine. The diamine-terminated hydrophilic polyimide, NTDA-BSPB, was prepared by the reaction of the NTDA (2.92 g, 10.9 mmol) and excess BSPB (5.08 g, 11.0 mmol) in *m*-cresol (40 ml). The NTDA-BSPB-*b*-DABA solution (1.0 g/10 ml of *m*-cresol) was added to the NTDA-BSPB solution. After a 24 h reaction, the solution was poured into methanol several times to completely remove the residual sulfonated diamine-terminated polyimide, NTDA-BSPB. In addition, the S-*bg*-PI as the sulfonated block-graft copolyimide was precipitated in ethyl acetate and recovered. Subsequently, the sulfonated block-graft copolyimides were dried in a vacuum oven at 150 °C for 15 h.

Other copolyimides, sulfonated random-graft copolyimide (S-*rg*-PI), sulfonated graft copolyimide (S-*g*-PI), and sulfonated block copolyimide (S-*b*-PI) were synthesized by similar procedure (see Supporting information for details).

2.3. Preparation of sulfonated copolyimide membranes

The sulfonated copolyimide membranes were prepared using a solvent-cast method. A 10 ml DMSO solution of the polyimide (0.4 g) was cast on a glass plate, and the plate was then placed in a vacuum oven at 110 °C for 24 h. The membrane was immersed in ethanol and deionized water for 4 h each, then acidified with a 0.1 M HCl solution for 4 h, and finally washed with deionized water for 4 h. The resulting membrane was dried in a vacuum oven at 80 °C for 24 h. The thickness of the membrane was approximately 50 μm.

2.4. Characterization of sulfonated copolyimide membranes

Thermal behavior of the polyimide membranes was evaluated by thermogravimetric analysis (TGA: Seiko TG/DTA60/60H, Tokyo, Japan) from room temperature to 600 °C at a heating rate of 10 °C min^{-1} in a nitrogen atmosphere.

The proton conductivity was measured using electrochemical impedance spectroscopy over the frequency range from 50 Hz to 500 kHz (Hioki 3532-50, Tokyo, Japan) as reported in previous papers [13,15]. The membranes (1.0×3.0 cm^2) and two blackened platinum plate electrodes were placed in a Teflon cell. The distance

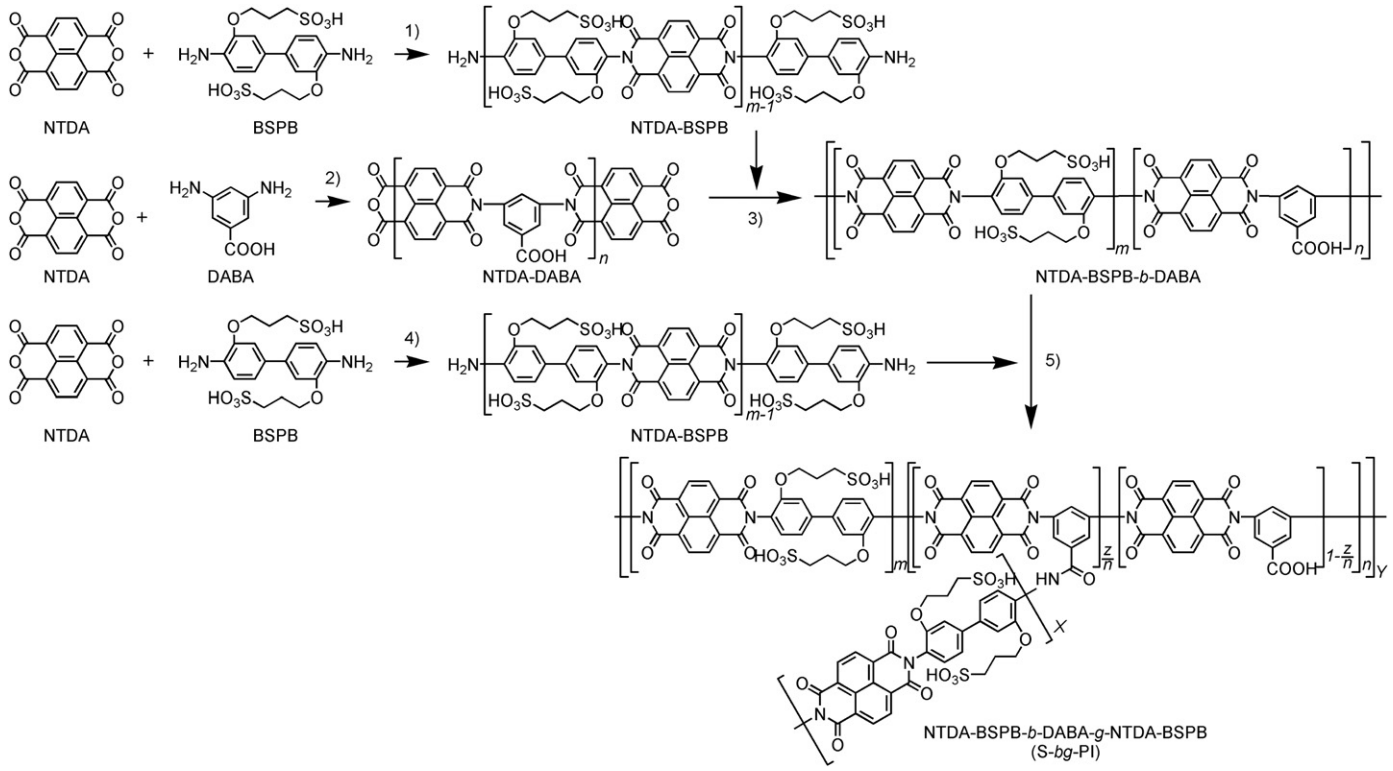

Scheme 1. Synthesis of the sulfonated block-graft copolyimide (S-*bg*-PI). 1) $N(C_2H_5)_3$, *m*-cresol, 120 °C, 24 h, 2) $N(C_2H_5)_3$, *m*-cresol, 120 °C, 24 h, 3) $N(C_2H_5)_3$, *m*-cresol, benzoic acid, 180 °C, 24 h, 4) $N(C_2H_5)_3$, *m*-cresol, benzoic acid, 120 °C, 24 h and 180 °C, 24 h, 5) $P(C_6H_5)_3$, pyridine, *m*-cresol, 180 °C, 24 h.

between the two electrodes was 1.0 cm. The cell was placed in a thermo-controlled humidity chamber to measure the temperature (from 90 to 30 °C) and relative humidity (from 98 to 30%RH) dependence of the proton conductivity.

Water uptake of the sulfonated copolyimide membranes was gravimetrically measured from the dried and humidified membranes [13]. The membranes were dried in a vacuum oven at 80 °C for 10 h and then immersed in liquid water at room temperature. After 24 h, the membrane was then wiped dry and quickly weighed. The water uptake was calculated using Eq. (1):

$$W(\%) = \frac{W_s - W_d}{W_d} \times 100 \quad (1)$$

where W_s and W_d are the weights of the wet and dry membranes, respectively.

Number of water molecules per sulfonic groups (λ) was calculated from the water uptake results using Eq. (2).

$$\lambda = \frac{n(H_2O)}{n\left(SO_3^-\right)} = \frac{WS}{18 \times IEC} \quad (2)$$

where $n(H_2O)$ is the H_2O molar number, $n(SO_3^-)$ is the SO_3 groups mole number, WS is the water uptake value by weight, IEC is the ion exchange capacity based on titration measurements, and 18 corresponds to the water molecular weight.

Acid concentration ($[H^+]$) of the membranes was determined according to Eq. (3) ref. [16]:

$$\left[H^+\right] = \frac{IEC \times W_d}{V_{wv}} \quad (3)$$

where W_d and V_{wv} are the weight of the dry membrane and the volume of the wet membrane, respectively.

The effective proton mobility (μ_{eff}) was then calculated from Eq. (4) ref. [16]:

$$\mu_{eff} = \frac{\sigma}{F[H^+]} \quad (4)$$

where F is Faraday's constant.

The gas permeability coefficients (P) of oxygen were measured with a high vacuum apparatus (Rika Seiki, Inc., K-315-H, Tokyo, Japan) [13,15]. The gas permeation measurements of the sulfonated copolyimide membranes were carried out from 25 °C up to 45 °C at 76 cmHg. The permeation parameters, diffusion coefficient (D) and solubility coefficient (S), of the sulfonated copolyimide membranes were calculated from

$$P = DS \quad (5)$$

$$D = \frac{L^2}{6\theta} \quad (6)$$

using the time lag, θ.

The hydrolysis stability was investigated by measuring the times that a membrane starts to break into pieces in water at 80 °C. The oxidative stability was measured by soaking in Fenton's reagent (30 ppm $FeSO_4$ in 30% H_2O_2) at 25 °C as an accelerated testing. The stability was evaluated by recording the time when membranes dissolved completely.

3. Results and discussion

3.1. Synthesis and characterization of the sulfonated block-graft copolyimide

The structures of the obtained sulfonated copolyimides were characterized by ^{1}H NMR. Fig. 2 shows the ^{1}H NMR spectra of NTDA-BSPB-*b*-DABA and S-*bg*-PI. The peaks of aromatic protons in NTDA-BSPB-*b*-DABA and S-*bg*-PI could be well assigned to the supposed chemical structures: Peaks at 8.9 and 8.8 ppm were assigned to aromatic proton in NTDA of S-*bg*-PI. Several peaks derived from BSPB moieties were observed from 7.7 to 7.4 ppm. Peaks for DABA were observed at 8.3 and 7.8 ppm. In addition, there was no peak derived

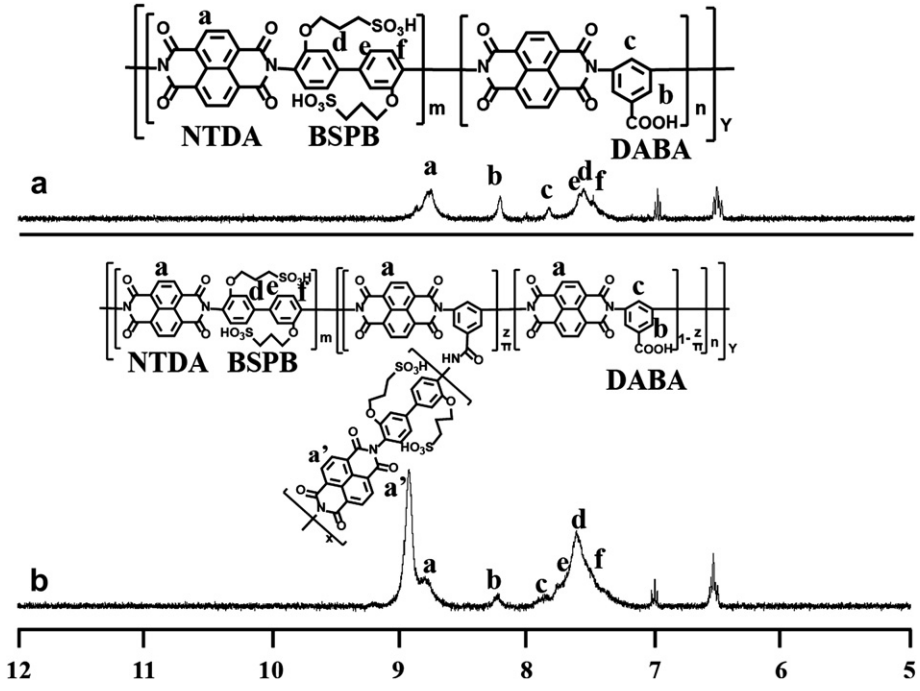

Fig. 2. ^{1}H NMR spectra of sulfonated NTDA-BSPB-*b*-DABA (a) and S-*bg*-PI (b).

from poly (amic acid), which is an intermediate of polyimide, at around 11 ppm, supporting that the novel sulfonated block-graft copolyimide was synthesized and the polymer main-chain was completely imidized. The integral ratio of NTDA/BSPB/DABA shown in Fig. 2(a) was 6.6/7.0/1.0, which led the ratio of hydrophilic segment (*m* in Fig. 2(a)) and hydrophobic segment (*n* in Fig. 2(a)) was 0.76/0.24. After the grafting reaction of the side-chain (NTDA-BSPB), the integral ratio of NTDA/BSPB/DABA changed to 17/19/1.0 shown in Fig. 2(b). Since the excess unreacted NTDA-BSPB was removed by precipitation purification, the increment of integral ratio of NTDA and BSPB units indicated that the NTDA-BSPB was grafted to the NTDA-BSPB-*b*-DABA as the side-chains. The grafting ratio of NTDA-BSPB side-chains onto NTDA-BSPB-*b*-DABA main-chain was calculated to be 1.5% from the NMR results. Ion exchange capacity (IEC) of S-*bg*-PI was determined by titration to give 2.51 meq g^{-1}, which gave close agreement with the IEC value (2.5 meq g^{-1}) calculated from the NMR results. Other sulfonated copolyimides, S-*rg*-PI, S-*g*-PI, and S-*b*-PI, were also obtained as completely imidized structures to possess similar IECs summarized in Table 1 (for synthetic details, see Supporting information).

Fig. 3 shows the thermogravimetric analysis (TGA) curves of NTDA-BSPB-*b*-DABA as the main-chain polymer, NTDA-BSPB as the side-chain polymer, and S-*bg*-PI. The curve of S-*bg*-PI was similar to that measured in NTDA-BSPB-*b*-DABA and NTDA-BSPB. The loss above 280 °C was due to the desulfonation from NTDA-BSPB-*b*-DABA, NTDA-BSPB, or S-*bg*-PI. In addition, the weight losses of sulfonic acid groups for the NTDA-BSPB-*b*-DABA, NTDA-BSPB, and S-*bg*-PI were 24%, 33%, and 30%, respectively, which were consistent with their IEC values. The weight loss above 550 °C was ascribed to the decomposition of the polymer main chain. The TGA curves of S-*rg*-PI, S-*g*-PI, and S-*b*-PI also displayed thermal stability similar to that of S-*bg*-PI (data not shown).

3.2. Proton conductivity of the sulfonated copolyimide membranes

Fig. 4(a) shows that S-*bg*-PI, S-*rg*-PI, and S-*g*-PI membranes demonstrated higher conductivities exceeding that of Nafion 117 at all temperatures, and their conductivities at 80 °C and 98%RH were 0.44, 0.43, and 0.45 S cm^{-1}, respectively, which were ca. 3 times more than that of Nafion 117 (Table 1). The proton conductivity of the four membranes at 80 °C and 98%RH decreased in the following order: S-*bg*-PI ≈ S-*rg*-PI ≈ S-*g*-PI > S-*b*-PI, indicating that proton conductivities were depend upon the molecular structures and morphologies; and the graft structures are more likely to affect the high proton conductivities than the block structures. On the other hand, the proton conductivity of the four membranes at 80 °C and 30%RH decreased in the following order: S-*bg*-PI > S-*b*-PI > S-*rg*-PI > S-*g*-PI, suggesting that the block-type polymer membranes show higher proton conductivity than the graft-type polymer membrane at a low humidity. As is apparent from Table 1, the activation energy of the proton conductivity (ΔEa_p) for the S-*bg*-PI membrane was almost similar to that for Nafion, indicating that the ionic domains in the S-*bg*-PI membrane might be well-interconnected as in Nafion. Therefore, the proton conductivity of the S-*bg*-PI membrane (0.44 S cm^{-1} at 80 °C and 98%RH) was one of the highest values in the other reported sulfonated polyimide membranes [14,17–22] though the IEC value of S-*bg*-PI was almost similar to these membranes.

Table 1
Ion exchange capacity (IEC), proton conductivity (σ), and activation energy for proton conductivity (ΔEa_p) of the sulfonated copolyimide membranes.

Polymer	IEC (meq g^{-1})	σ (S cm^{-1}) 80 °C, 98%RH	σ (S cm^{-1}) 80 °C, 30%RH	ΔEa_p (kJ mol^{-1})
S-*bg*-PI	2.51	0.44	1.0×10^{-3}	19
S-*rg*-PI	2.48	0.43	1.7×10^{-5}	24
S-*g*-PI	2.32	0.45	8.3×10^{-6}	30
S-*b*-PI	2.21	0.17	2.6×10^{-4}	28
Nafion 117	0.91	0.15	6.4×10^{-3}	21

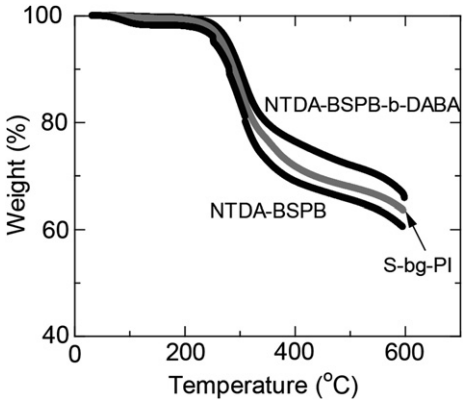

Fig. 3. Thermogravimetric analysis curves of S-*bg*-PI.

Fig. 4(b) shows the relative humidity dependence of the proton conductivities of the sulfonated copolyimide membranes at 80 °C. The conductivities of S-*bg*-PI membrane were similar to or higher than these of Nafion 117 from 70 to 98%RH. In general, the proton conductivities for most polymer electrolyte membranes based on the sulfonated polyimide is well known to significantly decrease compared to that determined in Nafion under low humidity conditions [19,20,22]. In this study, the conductivities of S-*rg*-PI and S-*g*-PI membranes were also much lower than Nafion 117 at the lower humidities. However, the S-*bg*-PI membrane indicated much higher conductivity than S-*rg*-PI and S-*g*-PI membranes, and its value was closer to that of Nafion 117 than those of other sulfonated copolyimides, S-*rg*-PI, S-*g*-PI, and S-*b*-PI, at the low humidities (Table 1).

As all of the sulfonated polyimide membranes possess similar IEC values (2.2–2.5 meq g^{-1}, Table 1), the proton conductivity differences must be derived from their polymer architectures. To elucidate the proton transport through the sulfonated polyimide membrane, the humidity dependence of the number of water molecules per sulfonic groups (λ) was investigated, in addition, the effective proton mobility (μ_{eff}) through the membranes was also estimated from the measured proton conductivity and the measured analytical [H^+] [22–24]. Fig. 5(a) revealed that the block main-chain structures in S-*bg*-PI and S-*b*-PI apparently improved water retention abilities than the NTDA-BSPB graft structures in S-*rg*-PI and S-*g*-PI did. In addition, S-*bg*-PI exhibited a higher μ_{eff} value than those measured in S-*rg*-PI and S-*g*-PI, as shown in Fig. 5(b). The high proton conductivity of S-*bg*-PI as seen in Fig. 4(a) and (b) might be responsible for the high water retention ability and proton mobility. In contrast, the μ_{eff} plot for S-*b*-PI was quite different from those for the graft-type copolyimide membranes. This might be due to the fact that the ionic domains induced in S-*b*-PI were quite different from that formed in the graft-type copolyimide membrane.

3.3. Gas permeability of the sulfonated copolyimide membranes

Table 2 summarizes the oxygen permeability coefficients (PO_2) of the sulfonated copolyimide membranes in the dry state at 35 °C and 76 cmHg. Although S-*b*-PI with high proton conductivity showed higher oxygen permeability than Nafion, the oxygen permeabilities of the graft-type polymer membranes, such as S-*bg*-PI, S-*rg*-PI, and S-*g*-PI, containing NTDA-BSPB side-chain structures showed significantly lower values than that of Nafion. In particular, the oxygen permeabilities of the S-*bg*-PI and S-*rg*-PI membranes were approximately 1–30th the value of Nafion, that is to say, these membranes had very excellent gas barrier property. The conventional polymer electrolyte membranes including Nafion, sulfonated

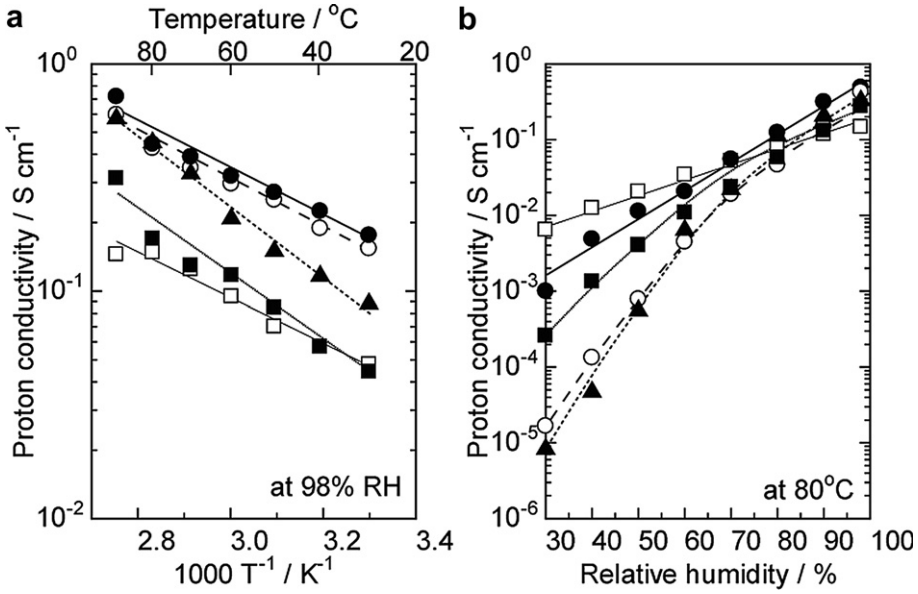

Fig. 4. (a) Temperature dependence (98%RH) and (b) relative humidity dependence (80 °C) of proton conductivity of sulfonated copolyimide membranes. (●) S-*bg*-PI, (○) S-*rg*-PI, (▲) S-*g*-PI, (■) S-*b*-PI, (□) Nafion 117.

polyimides [14,15,17–21], sulfonated poly(arylene ether)s [25–28], and sulfonated polyphenylenes [29] have comparable characteristics on their proton conductivity and oxygen permeability, however, the novel sulfonated polyimides, especially S-*bg*-PI and S-*rg*-PI, showed distinguishing properties that are their low gas permeabilities even though their high proton conductivities. As being apparent from Fig. 6, the proton and oxygen transports of their membranes greatly surpassed the most recent upper bounds of conventional and state-of-art PEMs. The significant low gas permeabilities of the novel sulfonated polyimide membranes are responsible for the reduced oxygen diffusion coefficients (DO_2), as is apparent from Table 2. We have reported that the oxygen molecule selectively transports through the hydrophobic domains in the proton exchange membrane [13]. For S-*bg*-PI or S-*rg*-PI, as the sulfonic acid groups were introduced among the hydrophobic domains, strong intermolecular interactions were produced in the membranes so that the gas diffusivity was remarkably suppressed.

The gas permeability generally increases with operating temperature; therefore the polymer electrolyte membrane is required to suppress the gas crossover at high temperature ranges. Here we compare the PO_2 values of the sulfonated copolyimide membranes and Nafion at 80 °C. As direct measurements of PO_2 values of the membranes at 80 °C was difficult due to our apparatus issue, PO_2 values at 80 °C were estimated from the experimentally calculated activation energy for their gas permeability coefficients (ΔEa_g). Nafion 117 indicated a high ΔEa_g value, and its PO_2 value at 80 °C was estimated to be 1.7×10^{-9} cm^3(STP) cm/(cm^2 sec cmHg), which is almost similar to the experimental value reported by Watanabe et al. [22]. On the other hand, the activation energy ΔEa_g of S-*bg*-PI, S-*rg*-PI, S-*g*-PI, and S-*b*-PI were much lower than that of

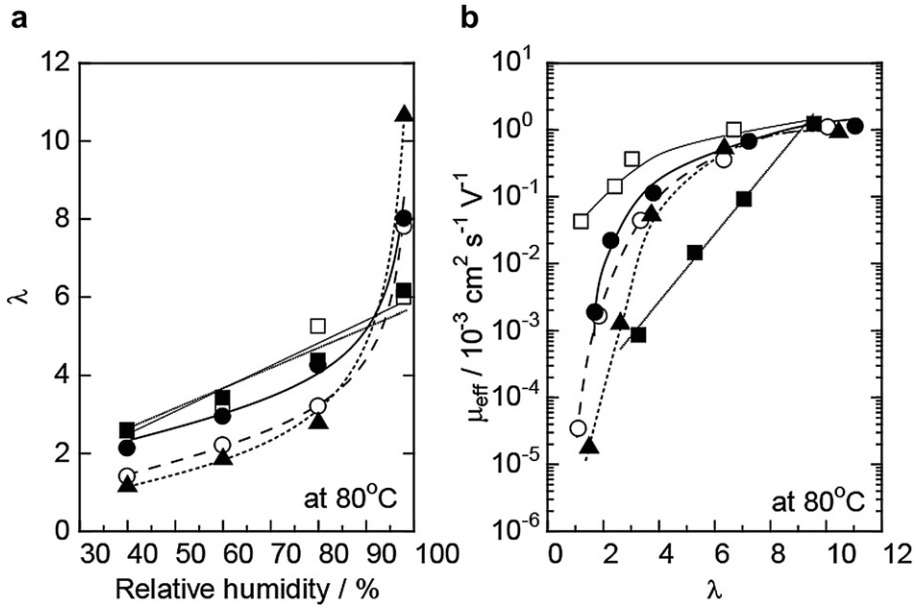

Fig. 5. (a) Relative humidity dependence of number of Water molecular per sulfonic group (λ) and (b) Proton mobility (μ_{eff}) of sulfonated copolyimide membranes. (●) S-*bg*-PI, (○) S-*rg*-PI, (▲) S-*g*-PI, (■) S-*b*-PI, (□) Nafion 117.

Table 2
Oxygen permeability coefficient (PO_2), diffusion coefficient (DO_2), solubility coefficient (SO_2), activation energy of oxygen permeability coefficient (ΔEa_g), apparent selectivity, and apparent selectivity ratio of the sulfonated copolyimide and Nafion membranes.

Polymer	PO_2	DO_2	SO_2	ΔEa_g (kJ mol^{-1})	Apparent selectivity	Apparent selectivity ratio
S-*bg*-PI	0.032	0.033	0.97	8.7	14	103
S-*rg*-PI	0.033	0.042	0.79	8.8	13	96
S-*g*-PI	0.25	0.34	0.75	11	1.8	13
S-*b*-PI	1.3	1.0	1.3	15	0.13	1
Nafion 117	1.1	4.6	0.23	49	0.13	1

PO_2: 10^{-10}(cm^3(STP) cm/(cm^2 sec cmHg)), DO_2: 10^{-8}(cm^2 sec^{-1}), SO_2: 10^{-2}(cm^3(STP)/(cm^3 cmHg)), Apparent selectivity = [Proton conductivity at 80 °C and 98% relative humidity/PO_2 at 35 °C and 76 cmHg]: 10^{10}(S sec cmHg cm^2(STP)), Apparent selectivity ratio = [Apparent selectivity (SPI)/Apparent selectivity (Nafion)].

Nafion. In particular, S-*bg*-PI and S-*rg*-PI membranes have exceedingly-small values less than 9 kJ mol^{-1}. The reason why the sulfonated copolyimide membranes showed low activation energies is considered that the sulfonated aromatic copolyimides have better thermal characteristics and lower temperature dependency of gas permeability than the perfluorinated aliphatic polymer electrolyte. The PO_2 values of the S-*bg*-PI membrane at 80 °C were estimated to be 4.7×10^{-12} cm^3(STP) cm/(cm^2 sec cmHg), which is three orders less than that of Nafion (1.7×10^{-9} cm^3(STP) cm/(cm^2 sec cmHg)).

As described above, most of polymer electrolytes have critical problems in realizing both high proton conductivity and low gas permeability of the fuel; that is, the polymer electrolyte membranes with high proton conductivity shows relatively high gas permeability. In order to make clear the differences of their characteristics, "apparent (proton/oxygen transport) selectivity" was established by dividing a proton conductivity value at 80 °C and 98%RH by an oxygen permeability coefficient value at 35 °C. The apparent selectivity values among the polymer electrolyte membranes were compared using "apparent selectivity ratio", which was standardized by the apparent selectivity value of Nafion. Since the PO_2 values of S-*bg*-PI and S-*rg*-PI were much lower than those of the other membranes, the apparent selectivity ratio of S-*bg*-PI and S-*rg*-PI were 103 and 96 times greater than that determined in Nafion.

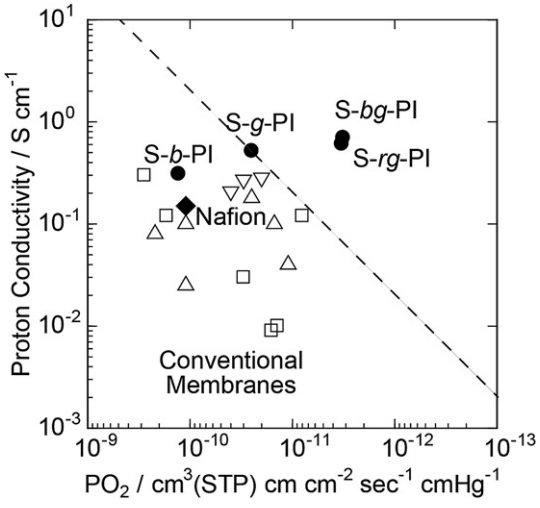

Fig. 6. Relationship between proton conductivity (at 80–90 °C and 90–98%RH) and oxygen permeability (at 25–40 °C and 76 cmHg) of (●) the novel sulfonated polyimide membranes and other previously reported polymer electrolyte membranes: (◆) Nafion, (□) sulfonated polyimides [13,17,18,22], (△) sulfonated poly(arylene ether)s [25–28], and (▽) sulfonated polyphenylenes [29].

Table 3
Hydrolysis and oxidative stabilities of sulfonated copolyimide membranes.

Polymer	Hydrolysis stability[a] (h)	Oxidative stability[b] (h)
S-*bg*-PI	>1000	3.0
S-*rg*-PI	>1000	3.5
S-*g*-PI	>1000	3.0
S-*b*-PI	>1000	3.0
Nafion 117	–	–

[a] The hydrolysis stability was measured by the time that the membranes dissolved in water at 80 °C.
[b] The oxidative stability was measured by the time that the membranes completely dissolved in Fenton reagent at 80 °C.

3.4. Chemical stabilities of the sulfonated copolyimide membranes

Finally, hydrolysis and oxidative stabilities of S-*bg*-PI, S-*rg*-PI, S-*g*-PI, and S-*b*-PI membranes were investigated under accelerated testing conditions in hot water and Fenton's reagent, respectively (Table 3). It is known that faster degradation for higher IEC membranes is reasonable due to the higher water uptake. Therefore, aromatic hydrocarbon PEM membranes bearing a large amount of sulfonic acid groups generally show poor membrane stabilities [8]. In contrast, S-*bg*-PI, S-*rg*-PI, S-*g*-PI, and S-*b*-PI showed high hydrolysis stabilities (stable in hot water for more than 1000 h) despite of their relatively high IECs. On the other hand, the oxidative stabilities of these membranes were almost similar (it takes 3–3.5 h to be fully dissolved in Fenton's reagent) regardless of polymer structures. It means that more proton conductive S-*bg*-PI and S-*rg*-PI still maintained similar oxidative stabilities to S-*g*-PI and S-*b*-PI, though the graft polymers had better proton conductive pathway, leading to higher diffusion of peroxide and the derived radical species degrades the polymer membranes. However, when compared to Nafion, the membrane stability of S-*bg*-PI or S-*rg*-PI is still insufficient for use in future fuel cell applications. The stability enhancement of the S-*bg*-PI membrane is now under considerations in our group and will be reported elsewhere.

4. Conclusion

A novel sulfonated block-graft copolyimide and other random-graft, graft, and block copolyimides were successfully synthesized. The novel copolyimide membranes, especially block-graft copolyimide membrane, showed high proton conductivity and low gas permeability. We considered that the high proton conductivity might be responsible for the high water retention ability and proton mobility, and that the strong intermolecular interaction formed by the sulfonic acid groups introduced among the hydrophobic domains remarkably suppressed the gas permeability. Though the membrane stabilities of the novel sulfonated block-graft copolyimide were insufficient for use in practical fuel cell applications, the outstanding low gas permeability and sufficient high proton conductivity of the novel membrane will promise to utilize future applications in fuel cell by improving the stabilities.

Acknowledgements

This work was partially supported by a grant (No.08004961-0) from NEDO, Japan and an ALCA grant from JST, Japan.

Appendix A. Supplementary material

Supplementary material associated with this article can be found, in the online version, at http://dx.doi.org/10.1016/j.jpowsour.2012.05.097.

References

[1] W. Vielstich, Handbook of Fuel Cells, Wiley, Chichester, England, 2009.
[2] L. Carrette, K.A. Friedrich, U. Stimming, Fuel Cells 1 (2001) 5–39.
[3] R. Borup, J. Meyers, B. Pivovar, Y.S. Kim, R. Mukundan, N. Garland, D. Myers, M. Wilson, F. Garzon, D. Wood, P. Zelenay, K. More, K. Stroh, T. Zawodzinski, J. Boncella, J.E. McGrath, M. Inaba, K. Miyatake, M. Hori, K. Ota, Z. Ogumi, S. Miyata, A. Nishikata, Z. Siroma, Y. Uchimoto, K. Yasuda, K. Kimijima, N. Iwashita, Chem. Rev. 107 (2007) 3904–3951.
[4] Q. Yan, H. Toghiani, J. Wu, J. Power Sources 158 (2006) 316–325.
[5] B.C.H. Steele, A. Heinzel, Nature 414 (2001) 345–352.
[6] J. Rozière, D. Jones, J. Annu. Rev. Mater. Res. 33 (2003) 503–555.
[7] M.A. Hickner, B.S. Pivovar, Fuel Cells 5 (2005) 213–229.
[8] P.M. Mangiagli, C.S. Ewing, K. Xu, Q. Wang, M.A. Hickner, Fuel Cells 4 (2009) 432–438.
[9] N. Karst, V. Faucheux, A. Martinent, P. Bouillon, J.Y. Laurent, F. Druart, J.P. Simonato, J. Power Sources 195 (2010) 1156–1162.
[10] F. Liu, B. Yi, D. Xing, J. Yu, H. Zhang, J. Memb. Sci. 212 (2003) 213–223.
[11] X. Cheng, J. Zhang, Y. Tang, C. Song, J. Shen, D. Song, J. Zhang, J. Power Sources 167 (2007) 25–31.
[12] M. Inaba, T. Kinumoto, M. Kiriake, R. Umebayashi, A. Tasaka, Z. Ogumi, Electrochim. Acta 54 (2009) 1076–1082.
[13] K. Yamazaki, H. Kawakami, Macromolecules 43 (2010) 7185–7191.
[14] N. Aasano, K. Miyatake, M. Watanabe, Chem. Mater. 16 (2004) 2841–2843.
[15] K. Yamazaki, M. Tanaka, H. Kawakami, J. Appl. Memb. Sci. Tech. 12 (2010) 7–17.
[16] O. Savard, T.J. Peckham, Y. Yang, S. Holdcroft, Polymer 49 (2008) 4949–4959.
[17] K. Tanaka, M.N. Islam, M. Kido, H. Kita, K. Okamoto, Polymer 47 (2006) 4370–4377.
[18] J. Saito, K. Miyatake, M. Watanabe, Macromolecules 41 (2008) 2415–2420.
[19] T. Suda, K. Yamazaki, H. Kawakami, J. Power Sources 195 (2010) 4641–4646.
[20] K. Yamazaki, Y. Tang, H. Kawakami, J. Memb. Sci. 362 (2010) 234–240.
[21] Z. Hu, Y. Yin, K. Okamoto, Y. Moriyama, A. Morikawa, Polymer 52 (2011) 2255–2262.
[22] J. Saito, M. Tanaka, K. Miyatake, M. Watanabe, J. Polym. Sci. Polym. Chem. 48 (2010) 2846–2854.
[23] T.J. Peckham, J. Schmeisser, M. Rodgers, S. Holdcroft, J. Mater. Chem. 17 (2007) 3255–3268.
[24] R. Takemori, H. Kawakami, J. Power Sources 195 (2010) 5957–5961.
[25] B. Bae, K. Miyatake, M. Watanabe, J. Memb. Sci. 310 (2008) 110–118.
[26] B. Bae, K. Miyatake, M. Watanabe, Macromolecules 42 (2009) 1873–1880.
[27] B. Bae, K. Miyatake, M. Watanabe, Macromolecules 43 (2010) 2684–2691.
[28] E. Fontananova, F. Trotta, J.C. Jansen, E. Drioli, J. Memb. Sci. 348 (2010) 326–336.
[29] S. Seesukphronrarak, K. Ohira, K. Kidena, N. Takimoto, C.S. Kuroda, A. Ohira, Polymer 51 (2010) 623–631.